American Mineralogist, Volume 65, pages 766-769, 1980

Defects along kyanite-staurolite interfaces

HANS-RUDOLF WENK

Department of Geology and Geophysics, University of California
Berkeley, California 94720

Abstract

The note describes (100) stacking faults in kyanite from a staurolite–kyanite intergrowth with a displacement vector $\mathbf{R} = \frac{1}{2}\mathbf{b}$. Diffraction spots $k \neq 2n$ are streaked and only with those reflections stacking faults are in contrast, which is interpreted as due to a displacement of $\frac{1}{2}\mathbf{b}$ on the (100) faults. This produces groups of two corner-sharing tetrahedra. If stacking faults occur periodically superstructures develop with a doubled or threefold a axis. These faults are frequently combined with lamellar microtwins adjacent to the kyanite–staurolite interface.

Kyanite and staurolite are two silicate minerals which are structurally closely related. Staurolite can be viewed as kyanite (Al_2SiO_5) with inserted layers which contain Fe in tetrahedral sites and have a composition AlO–OH–2FeO (Fig. 1). The interface is nearly coherent, with (010) of staurolite corresponding to (100) of kyanite (Naray-Szabo, 1929; Naray-Szabo *et al.*, 1929; Burnham, 1963). The two minerals often occur as crystallographic intergrowths, including the famous specimens from the Alpe Sponda in the Swiss Alps (*e.g.* Henriques, 1956; Juurinen, 1956). I decided to study these interfaces with the transmission electron microscope (TEM), aiming to find superstructure variations in staurolite or submicroscopic intergrowths of kyanite and staurolite. Staurolite was not very interesting. The homogeneous crystals are orthorhombic without superstructure reflections (Fig. 2b). The interface between staurolite and kyanite was found to be coherent with a few misfit dislocations (Fig. 2a). In the diffraction pattern b^* of staurolite corresponds to a^* of kyanite (Fig. 2c). Kyanite, however, displayed a whole spectrum of complications in the vicinity of the staurolite contact. Figure 3 shows a variety of $hk0$ selected-area electron diffraction patterns (SAD): (a) normal kyanite, (b) kyanite with streaks for k odd; (c) streaks as in (b) but with additional reflections for k odd, causing doubling of a; (d) similar to (c) but with sharp additional reflections; and (e) a threefold a lattice constant with extra reflections and satellites for k odd. SAD's (b–e) were obtained on areas about 5000Å in diameter which show planar defects (b and Fig. 4a) and lamellar structures (c–e and Fig. 4b,c) parallel to (100). The size of the electron beam was therefore too large to isolate the lamellar phase and all patterns must be regarded as composites.

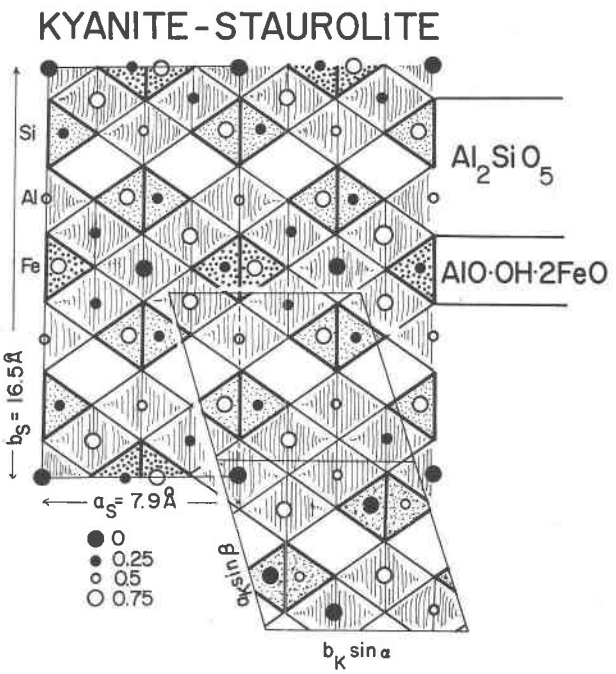

Fig. 1. z-axis projection of the structure of staurolite; shown in the lower right corner is an epitaxial intergrowth with kyanite.

Fig. 3 Selected-area electron diffraction patterns of kyanite. (a) Normal kyanite. (b) Kyanite with stacking faults (compare Fig. 4a). Superstructures in kyanite with diffuse additional reflections (c), sharp reflections mainly due to twinning (d), and superstructure reflections with satellites (e). (f) shows several layers of the coherent reciprocal lattice. [Camera length for (e) is about 2 times larger and for (f) about 3 times shorter than in (a–d).]

0003–004X/80/0708–0766$02.00

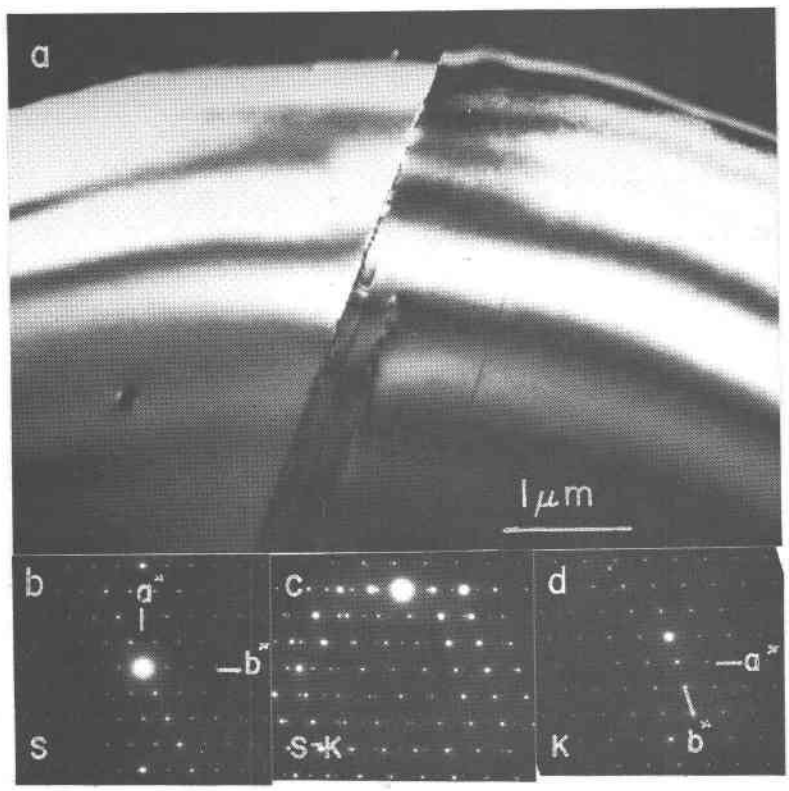

Fig. 2. Staurolite–kyanite interface in a crystal from Alpe Sponda. (a) Darkfield electron micrograph illustrating staurolite (left), the interface with strain contrast and misfit dislocations (center), and kyanite (right). Notice faults in kyanite. (b–d) SAD's of corresponding areas.

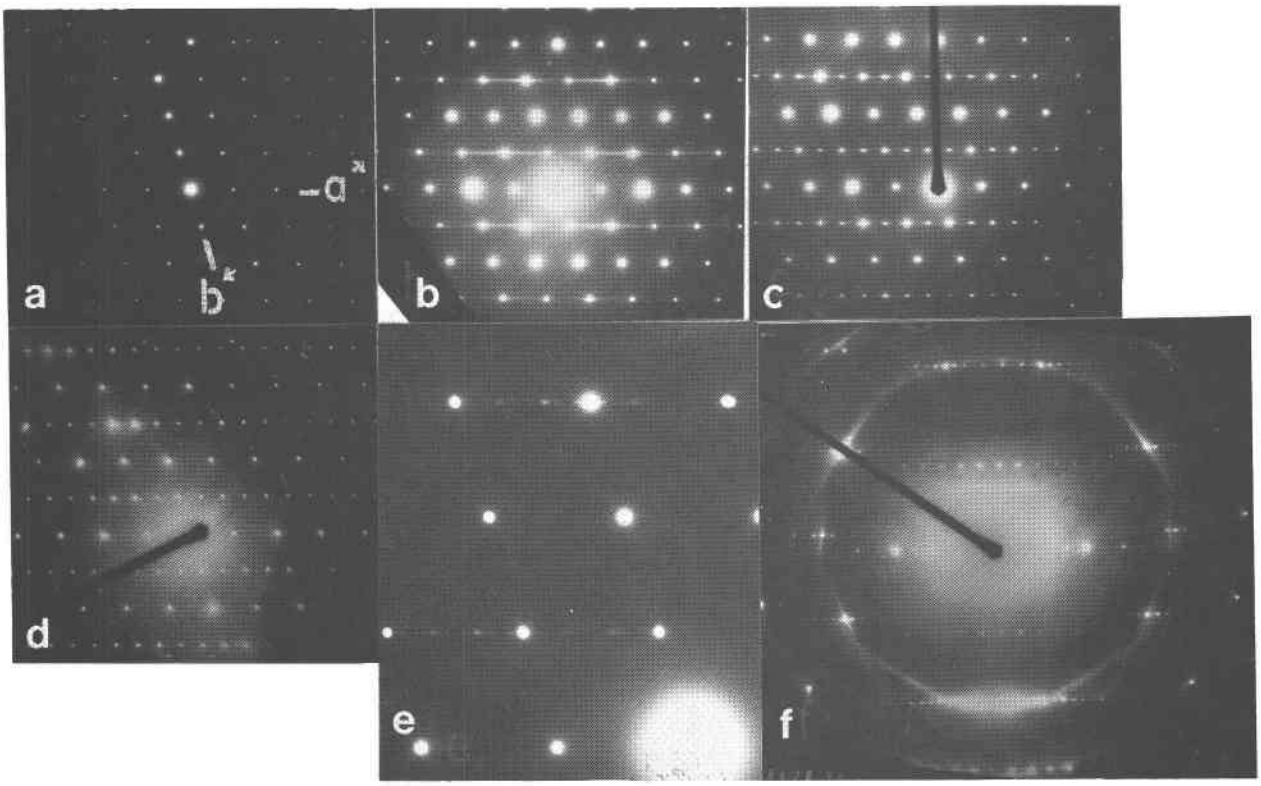

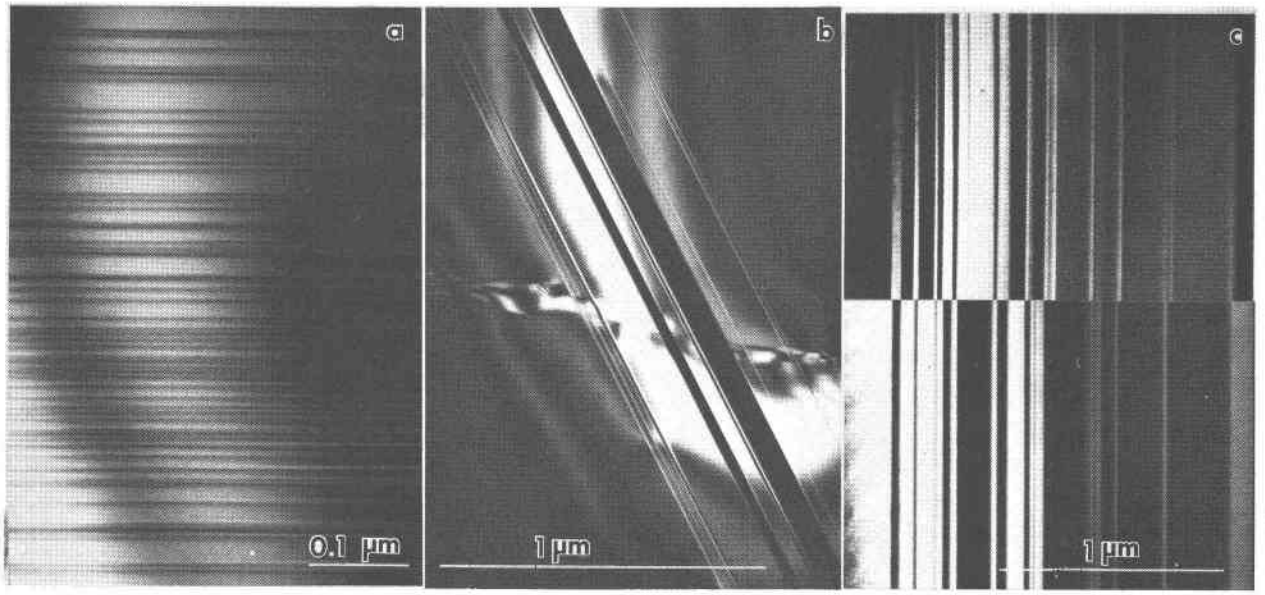

Fig. 4. Darkfield electron micrographs of microstructures in kyanite. (a) Stacking faults; (b) narrow bright lamellae are (100) microtwins (compare SAD in Fig. 3c–e); (c) contrast reversal in microtwins with host and twin reflections operating.

In the following paragraphs a structural model is proposed for these defects. The interpretation relies heavily on the analogy with wollastonite, which shows striking similarity (Wenk *et al.*, 1976). Let us first consider well-separated faults which are in contrast in darkfield with streaked k = odd reflections and out of contrast with k = even reflections which are sharp (Fig. 4a). Contrast experiments ($\mathbf{g} \cdot \mathbf{R}$) suggest that they are stacking faults with a fault vector $\mathbf{R} = \frac{1}{2}\mathbf{b}$. This is a plausible vector in the kyanite structure, in which oxygen atoms form layers parallel to (100) and are arranged in a pattern which repeats twice along b (Fig. 1). Application of the fault vector will join two tetrahedra and link them to form groups of two across the fault plane (Fig. 5g). If these stacking faults are periodic they produce a new superstructure. This is often the case over short distances, which can be seen in Figure 4a, and in coherent diffraction patterns such as those in Figure 3c,e which are indicative of superstructures. The systematic extinctions with fractional h for k = 2n arise because the $\frac{1}{2}\mathbf{b}$ translation effectively averages top and bottom halves of unit cells viewed along x.

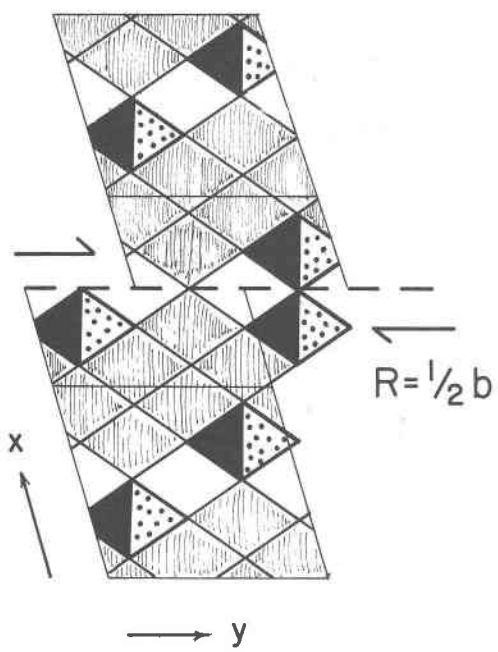

Fig. 5. Structure along a $\mathbf{R} = \frac{1}{2}\mathbf{b}$ (100) stacking fault viewed in a z-axis projection.

The strong contrast reversal across the lamellar structures in the darkfield photomicrographs Figures 4b and c is reminiscent of twinning. (100) twinning is common in kyanite because of pseudosymmetry (cos $\gamma^* \approx a^*/2b^*$). In the $hk0$ diffraction patterns k = 2n reflections almost coincide, as is shown in Figure 3d. Figure 4c shows contrast reversal in corresponding darkfield images of the same area with reflections from both twin and host operating. But microtwinning cannot account for all the SAD's (b, c, e) in Figure 3. Streaking in those patterns is only observed in k = odd layers. In microtwins with only rotational variants it would affect all reflections. This suggests that twinning is combined with (100) stacking faults

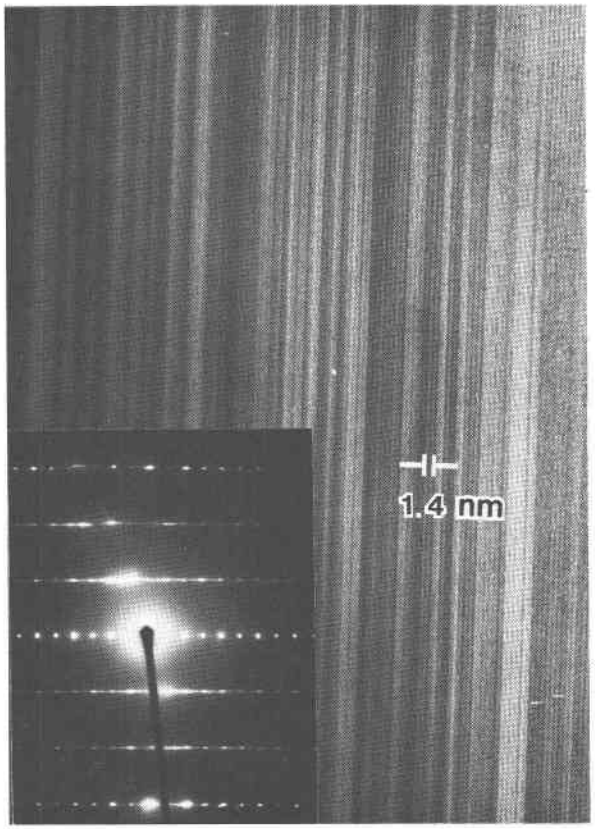

Fig. 6. Lamellae of 14Å chlorite in kyanite. Note the high density of stacking faults.

and that twin planes are glide planes with a ½**b** glide component. It is surprising that no reflections are split. Even high layers form a single coherent lattice (Fig. 3f).

Stacking faults and microtwins have been observed in three different kyanite–staurolite intergrowths, always in the immediate vicinity of the interface. Neither defect could be found further inside kyanite, and they are therefore thought to be characteristic of the intergrowth. As kyanite grows it has to adjust to the different stacking order from staurolite, and this is the cause for a high change of stacking defects. Possibly there is also some chemical heterogeneity in the transition zone. Energy-dispersive X-ray analyses inside the TEM suggest some concentrations of Fe in the lamellar structures, but the electron beam is too large to get an accurate analysis on a single lamella.

There are other complexities in the vicinity of the staurolite–kyanite interface. Lamellae of 14Å chlorite exist in kyanite with (100) kyanite parallel to (001) chlorite. Chlorite is riddled by stacking faults, as indicated by diffuse streaks for $k \neq 3n$ in the diffraction pattern (Fig. 6, inset) and in lattice fringe resolution micrographs (Fig. 6). The chemical analysis gives in weight units Mg = 0.5, Al = 1.5, Fe = 0.8, normalized to Si = 1. The chlorite mineral is amazingly resistant to electron beam damage.

Acknowledgments

I am indebted to Dr. J. Arnoth, Naturhistorisches Museum, Basel, for providing the specimens and remembering the summer of 1960 when I visited with him in Alpe Sponda where the specimens were collected. The experimental work was done on a JEM 100C transmission electron microscope provided by NSF grant EAR 77-00127. Photographic work by J. Hampel is gratefully acknowledged. Constructive comments by a critical reviewer are greatly appreciated.

References

Burnham, C. W. (1963) Refinement of the crystal structure of kyanite. *Z. Kristallogr., 118,* 337–360.

Henriques, A. (1956) The alkali content of kyanite. *Ark. Mineral. Geol., 2,* 271–274.

Juurinen, A. (1956) Composition and properties of staurolite. *Ann. Acad. Sci. Fennicae,* Ser. A III. Geol.–Geogr., No. 47.

Naray-Szabo, St. (1929) The structure of staurolite. *Z. Kristallogr., 71,* 103–116.

———, W. H. Taylor and W. W. Jackson (1929) The structure of cyanite. *Z. Kristallogr., 71,* 117–130.

Wenk, H. R., W. F. Müller, N. A. Liddell and P. P. Phakey (1976) Polytypism in wollastonite. In H. R. Wenk, Ed., *Electron Microscopy in Mineralogy,* p. 324–331. Springer, Heidelberg.

Manuscript received, November 20, 1978;
accepted for publication, December 14, 1979.